Journal of Applied Informatics and Computing (JAIC)
Vol.10, No.3, June 2026, pp. 2198~2208
e-ISSN: 2548-6861

Spatiotemporal Analysis of Peatland Fire Hotspots and Fire Intensity in Riau Province Using MODIS–VIIRS Multisensor Satellite Data

Najwa Ratu Afi[1], Ramadhan Rakhmat Sani[2]**, Ricardus Anggi Pramunendar[3]*, Nurul Anisa Sri Winarsih[4]*, Ika Novita Dewi[5]***
**Faculty of Computer Science, Universitas Dian Nuswantoro, Semarang, Indonesia
*Intelligent Distributed Surveillance and Security (IDSS), Universitas Dian Nuswantoro, Semarang, Indonesia
112202206896@mhs.dinus.ac.id [1], ramadhan_rs@dsn.dinus.ac.id [2], ricardus.anggi@dsn.dinus.ac.id [3], nurulanisasw@dsn.dinus.ac.id [4], ikadewi@dsn.dinus.ac.id [5]

Article Info

Article history:

Received 2026-03-19
Revised 2026-04-21
Accepted 2026-04-30

Keyword:

Peatland fire hotspots, Spatiotemporal analysis, MODIS–VIIRS multisensor data, Remote sensing,Fire monitoring

ABSTRACT

Peatland fires in Riau Province frequently occur during the dry season and contribute significantly to regional haze, environmental degradation and carbon emissions. Effective monitoring of these fires remains challenging due to their widespread distribution and varying intensity across peatland areas. This research aims to analyze the spatiotemporal characteristics of peatland fire hotspots in Riau Province using multisensor satellite observations from the NASA Fire Information for Resource Management System (FIRMS). The dataset integrates Moderate Resolution Imaging Spectroradiometer (MODIS) and Visible Infrared Imaging Radiometer Suite (VIIRS) data from the Suomi-NPP, NOAA-20 and NOAA-21 satellites. After applying filtering criteria of confidence ≥70% and Fire Radiative Power (FRP) ≥5 megawatts (MW), a total of 7,297 significant hotspots were identified during the July–October 2025 dry season. The results show that fire activity peaked in July with a maximum daily FRP of 25,611 MW and a monthly total of 65,120 MW, followed by a decline in September and a slight increase in October. The FRP distribution was highly right-skewed, with an average value of 13.2 MW, while the most intense hotspots reached 189.4 MW. Estimated carbon dioxide (CO_2) emissions reached approximately 122,472 tons, indicating substantial environmental impacts. Spatial clustering and persistence analysis revealed several high-risk peatland zones with repeated fire occurrences. These findings demonstrate the importance of multisensor satellite monitoring for improving early fire detection, emission assessment and disaster mitigation strategies in peatland regions.

I. INTRODUCTION

Wildfires and peatland fires represent one of the most critical environmental challenges worldwide due to their long-lasting ecological and climatic impacts [1]. Peat ecosystems store enormous amounts of organic carbon accumulated over thousands of years, making them highly sensitive to disturbance and combustion. When peatlands burn, they release large quantities of greenhouse gases and aerosols that significantly influence atmospheric composition and global climate dynamics [1].

Recurring peatland fires during the dry season are one of the most critical environmental problems in Indonesia, especially on the island of Sumatra, with Riau Province being a particularly vulnerable area [2]. These conditions lead to significant greenhouse gas emissions, air quality degradation, and long-term ecosystem damage, including soil structure degradation and land subsidence. Beyond the burning period, peat fires also induce post-fire hydrological changes, reducing water retention capacity, altering surface flow patterns, and increasing flood vulnerability during subsequent rainy seasons [3], [4]. These impacts are further exacerbated by transboundary haze, which causes economic

losses and public health burdens, particularly in urban areas [4]. These impacts are exacerbated by transboundary haze, which causes financial losses and health burdens, especially in urban areas [4]. Therefore, peatland fires need to be understood as a multidimensional phenomenon that goes beyond the issue of fire itself.

Monitoring peatland fire dynamics requires approaches capable of covering large and often inaccessible areas. In this context, satellite-based remote sensing is a very effective tool, particularly through the use of active hotspot data derived from the Moderate Resolution Imaging Spectroradiometer (MODIS) and Visible Infrared Imaging Radiometer Suite (VIIRS) sensors [3]. Hotspot products from NASA Fire Information for Resource Management System (FIRMS) enable consistent monitoring of fire events on a regional to global scale [5]. The Fire Radiative Power (FRP) parameter is widely used as a quantitative indicator of fire intensity due to its strong correlation with biomass consumption and carbon emissions across various vegetation types [6], [7], [8]. Advances in polar-orbiting sensors, particularly the improved temporal resolution of VIIRS, have further enhanced the reliability of FRP for near real-time monitoring of high-intensity fires in tropical peat ecosystems [9]. Furthermore, findings of increased fires in Riau Province are consistent with the national trend of drought amplification of up to 60% in southern Indonesia, which triggers hazards such as wildfires [10].

Although research on Indonesian peat fires has advanced, most studies primarily focus on ecological impacts, emissions, and burned-area mapping, with limited attention to temporal dynamics, fire intensity, and energy accumulation. Conventional approaches relying on static hotspot counts or pre-2020 datasets often overlook time-series FRP accumulation, extreme thresholds (P90/P95), and late-dry-season energy buildup. This limitation reduces the ability to capture the dynamics of high-intensity fires and their potential contribution to post-fire hydrological risks, particularly in tropical peatland regions such as Riau Province [11]. Rewetting has reduced extreme fire frequency by up to 40% in Riau Province [12], yet multisensor time-series links to secondary seasonal hazards remain underexplored. As a result, the dynamic relationship between accumulated fire energy, spatial concentration of intense hotspots and post-fire hydrological vulnerability remains insufficiently understood, particularly in tropical peatland regions such as Riau Province.

This research proposes a multisensor FRP-based analytical framework that integrates fire intensity, temporal accumulation, and spatial persistence. By capturing the disproportionate contribution of high-intensity fires and identifying late-season energy buildup, this approach provides a more comprehensive understanding of fire severity, emission dynamics, and potential post-fire hydrological impacts in tropical peatland ecosystems. This gap reduces the ability to fully capture the dynamics of high-intensity peat fires and their environmental impacts.

This research analyzes peat fires with a confidence level ≥70% and FRP ≥5 MW in Riau Province during July–October 2025 using MODIS and VIIRS multisensor data from NASA FIRMS [13]. The main contributions are:
(1) Time-series analysis of daily hotspots and accumulated FRP, identifying 7,297 significant hotspots and extreme fire episodes using P90/P95 thresholds, (2) Spatial analysis using grid-based fire persistence and monthly FRP distribution to detect high-intensity fire clusters in coastal peatlands, (3) Exploratory assessment of post-fire flood vulnerability linked to accumulated FRP, including an estimated 122 kt CO_2 equivalent emissions. This research emphasizes an energy-based fire characterization approach, enabling a more comprehensive interpretation of fire intensity, emission potential, and spatial persistence compared to conventional hotspot-count methods.

The structure of this research is organized systematically. Chapter II presents the methods, which include data collection, preprocessing, selection of main peatland hotspots, spatial and temporal analysis and statistical analysis and emission estimation. Chapter III presents the results and discussion, while Chapter IV provides the conclusion, summarizing the main findings and recommendations.

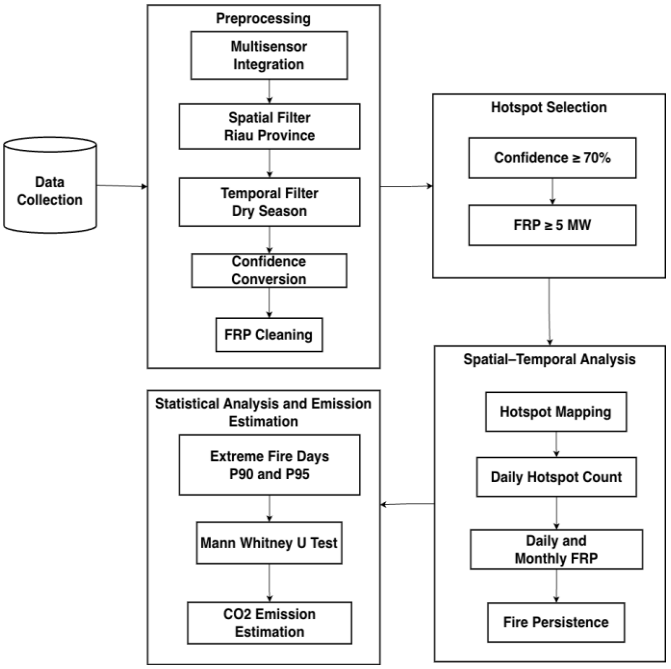

Figure 1. Research stages

II. METHODS

This research adopts a remote sensing–based analytical framework to examine the spatial and temporal dynamics of peatland fires in Riau Province during the 2025 dry season. Multisensor hotspot data from NASA FIRMS were

processed through a structured workflow (Figure 1) to identify high-intensity fire events across spatial and temporal scales.

Overall, this research methodology has five main stages: (1) Data Collection from NASA FIRMS Multisensor, (2) Preprocessing, (3) Hotspot Selection, (4) Spatial–Temporal Analysis, and (5) Statistical Analysis and Emission Estimation.

A. Data Collection

Fire activity data were obtained from NASA Fire Information for Resource Management System (FIRMS) at https://firms.modaps.eosdis.nasa.gov/download/ on December 22, 2025. The dataset integrates archival-quality fire products from MODIS Collection 6.1 and VIIRS Suomi NPP, VIIRS NOAA‑20, with near-real-time (NRT) observations from VIIRS NOAA‑21, ensuring complete fire detection coverage during the research period from July to October 2025 [3]. The spatial scope of this research is limited to Riau Province, located in central Sumatra, Indonesia. The analysis area is defined using a geographic bounding box of approximately 99.5°–103.5°E longitude and −1.5°–2.5°N latitude. This region was selected because it contains extensive tropical peatlands that are highly susceptible to seasonal fires during the dry season [2].

Archival data undergo more comprehensive processing, resulting in higher accuracy but with typical delays of 3–6 months, whereas NRT data provide low-latency observations for recent fire events. To focus on significant fire activity and reduce potential false detections, only hotspots with a confidence level ≥70% and FRP ≥5 MW were retained for further analysis [13]. This integration enhances detection reliability in cloud-prone tropical regions and facilitates robust spatiotemporal analysis, such as utilizing active fire products to determine confidence levels in burned area mapping [3].

The NASA FIRMS active fire dataset includes key variables describing detected thermal anomalies. These include acquisition date (acq_date), latitude and longitude for hotspot locations, confidence indicating the probability of a true fire detection and Fire Radiative Power FRP (MW), which represents the radiative energy released by the fire [3]. These variables describe the location, timing, and relative intensity of detected fire events.

To illustrate the data characteristics, the MODIS archive file contains 423,815 records, covering the entire July-October 2025 period in the downloaded dataset. This data shows moderate FRP values and varying confidence levels, reflecting its suitability for large-scale fire detection. The oldest and most recent sample records are shown in Table I, highlighting the typical FRP range and confidence level variation across global coordinates.

TABLE I
SAMPLE DATA FROM MODIS (COLLECTION 6.1 - ARCHIVE)

acq_date	latitude	longitude	confidence	frp
2025-07-01	42.9114	143.2588	44	7.9
2025-07-01	36.1819	139.1601	67	6.2
2025-07-01	35.0281	136.8662	0	9.3
2025-07-01	-12.6474	130.6096	80	39.1
2025-07-01	-12.6367	130.6009	72	24.7
…	…	…	…	…
2025-08-31	51.9205	48.0618	85	18.3

In addition to MODIS data, there is also a VIIRS S-NPP archive file consisting of 4,456,900 records, covering the entire period from July to October 2025 in the dataset provided. This file shows lower FRP values in the initial sample, which is typical for small fires that started and ended in late August, reflecting a delay in archive processing, as shown in Table II.

The NOAA-20 VIIRS archive file contains 4,512,592 records, which completely covers the period from July to October 2025 according to the download. This file records higher FRP values in several detections, indicating sensitivity to moderate to large fires, but ends in August due to archive delays, which can be seen in Table III.

TABLE II
SAMPLE DATA FROM VIIRS S-NPP (ARCHIVE)

Acq_Date	Latitude	Longitude	Confidence	FRP
2025-07-01	17.86784	33.83808	n	0.96
2025-07-01	13.51761	21.23083	n	0.41
2025-07-01	13.47416	13.99066	n	0.78
2025-07-01	12.89092	14.20371	n	2.27
2025-07-01	12.89051	14.20695	n	1.19
…	…	…	…	…
2025-08-31	-32.93733	18.76106	n	1.38

TABLE III
SAMPLE DATA FROM VIIRS NOAA-20 (ARCHIVE)

Acq_Date	Latitude	Longitude	Confidence	FRP
2025-07-01	70.3817	68.38053	n	3.44
2025-07-01	64.90432	75.52522	n	35.56
2025-07-01	4.90911	75.51754	n	43.29
2025-07-01	62.88909	73.60247	n	16.22
2025-07-01	69.26551	57.28759	n	3.35
…	…	…	…	…
2025-08-31	-33.96921	18.57942	n	0.49

Finally, the VIIRS NOAA-21 NRT file contains 7,819,028 records, providing the most complete coverage up to October 31, 2025. It displays consistent low-to-medium FRP values, leveraging VIIRS's higher resolution for detecting fragmented or smoldering fires. Sample records in Table IV

highlight its extended temporal span and uniform nominal confidence in early detections.

TABLE IV
SAMPLE DATA FROM VIIRS NOAA-21 (ARCHIVE)

Acq_Date	Latitude	Longitude	Confidence	FRP
2025-07-01	69.26582	57.28395	n	3.57
2025-07-01	70.38165	68.37774	n	4.71
2025-07-01	65.76380	24.18618	n	7.27
2025-07-01	65.77007	24.19186	n	3.64
2025-07-01	64.66412	21.28027	n	4.44
…	…	…	…	…
2025-10-31	-34.03355	22.42895	n	1.21

To evaluate the contribution of each data source, aggregation was performed after applying spatial, temporal, and intensity filters. These include the Riau Province boundary, the July–October 2025 period, and thresholds of confidence ≥70% and FRP ≥5 MW.

The confidence threshold was applied to reduce false-positive detections, while the FRP threshold excludes low-intensity fires with minimal contribution to total radiative energy. Although these thresholds are widely used, no formal sensitivity analysis was conducted. Therefore, the selection remains empirical and is acknowledged as a limitation of this research. The results are summarized in Table V. Each data source is compared based on raw records, total FRP (MW), number of significant hotspots, and percentage contribution to total radiative energy. This table shows that VIIRS sources, particularly NOAA-20 and NOAA-21, contribute significantly to the number of significant hotspots and total radiative energy in the research area, in line with the finer spatial resolution and detection sensitivity of VIIRS to fragmented fires on tropical peatlands [6].

TABLE V
COMPARISON OF FIRMS SOURCE DATA

Source	Raw Records	Total FRP	Total FRP (MW)	Hotspots	FRP
nrt_J2V-C2	7819028	2302	31852.6	31.5	25.7
archive_J1V-C2	4512592	1963	30744.9	26.9	24.8
archive_SV-C2	4456900	1872	24988.3	25.7	20.2
archive_M-C61	423815	504	24796.2	6.9	20.0
nrt_M-C61	1264065	231	6587.3	3.2	5.3
nrt_J1V-C2	3594102	223	2497.7	3.1	2.0
nrt_SV-C2	3754484	202	2362.2	2.8	1.9

The FRP column shows the percentage contribution to total radiative energy. The total value is calculated after deduplicating detections between sources. The FIRMS data set has been effectively applied to spatio-temporal fire monitoring and hotspot-pollution correlation analysis in Indonesian peatlands, as shown in a research linking vegetation fires to carbon monoxide emissions [14]. This supports the reliability of the data set in investigating the dynamics of peatland fires in Riau Province through the multisensor integration used in this research.

B. Preprocessing

Following data collection from NASA FIRMS, preprocessing was performed to focus the analysis on significant fire events using strict selection criteria. Multisensor integration was performed by harmonizing spatial and temporal differences between MODIS (±1 km) and VIIRS (±375 m). All hotspot detections were resampled into a unified 0.1° spatial grid and temporally aligned based on acquisition time. To minimize duplicate detections across sensors, a deduplication process was applied using a spatial threshold of <1 km and a temporal window of <1 hour. This ensures that multiple observations of the same fire event are counted only once during aggregation.

Following multisensor integration, a series of filtering steps were applied to refine the dataset. Spatial filtering was applied to retain only hotspots within the administrative boundary of Riau Province. Temporal filtering limited the dataset to July–October 2025, corresponding to the peak dry season [2]. Only hotspots with confidence ≥70% were retained to reduce false-positive detections [13].

Additionally, hotspots with FRP <5 MW were excluded to remove low-intensity detections and focus on fires with significant radiative energy and emission potential. This threshold is widely applied in tropical peat fire studies to capture fires that significantly contribute to air pollution and emissions [15]. Although no formal sensitivity analysis was conducted, the threshold selection remains empirical. Hotspots were further constrained to areas with peatland dominance >50% based on spatial overlay with peatland distribution maps. This approach is consistent with peatland-focused fire studies and supports the prioritization of vulnerable peat areas in fire prevention and restoration strategies [16]. All preprocessing steps were designed to ensure methodological transparency and reproducibility of the analysis.

C. Hotspot Selection

After the preprocessing stage of fire hotspot data, the selection of main peatland hotspots was carried out to focus the analysis only on significant events relevant to the characteristics of tropical peat fires. In this research, main hotspots refer to fire detections that meet two primary criteria including a confidence level ≥70% and FRP ≥5 MW within the spatial boundary of Riau Province. This step aims to ensure high data validity by minimizing detection errors and highlighting relatively high-intensity hotspots that contribute significantly to emissions. Hotspots were selected

if they had a confidence level of at least 70% in accordance with common practice in peatland fire monitoring in Indonesia to reduce false positives from MODIS data [13]. Furthermore, hotspots with a FRP value below 5 MW are excluded so that the analysis focuses on fires with more representative emission potential and intensity, as is often used in tropical peatland fire studies. The FRP ≥5 MW threshold was chosen as a methodological filter to prioritize active combustion with significant energy release. The threshold of 5 MW was selected because FRP values above this level generally represent active biomass burning with measurable radiative energy release, making them more suitable for assessing fire intensity and potential atmospheric emissions in peatland environments [6]. This approach allows for more accurate capture of fire signals without being disturbed by weak or small detections.

Whereas the third criterion requires hotspots to be located in areas with more than 50% peatland dominance based on overlay with peatland maps to prioritize locations where peatland fire characteristics dominate. Peatland areas were identified through spatial overlay between hotspot coordinates and regional peatland distribution maps derived from national peatland geospatial datasets. The >50% dominance threshold was applied as a custom spatial proxy to ensure majority peat coverage at hotspot locations. Peatland fires are significantly different from mineral soils, particularly in terms of longer burning duration and greater carbon emissions due to the burning of sub-surface peat layers [1]. By focusing on areas dominated by peat, the analysis becomes more accurate in describing the impact of emissions and the dynamics of fires that are characteristic of this ecosystem. Overall, this selection process produces a clean, valid hotspot dataset that is ready for further analysis, such as spatial mapping or post preprocessing emission estimates.

D. Spatial–Temporal Analysis

This grid-based approach enables the identification of spatial clustering patterns and persistent fire-prone zones, serving as a simplified proxy for clustering analysis in the absence of more computationally intensive spatial clustering algorithms. This spatial and temporal analysis was conducted after the selection process for major peatland hotspots was completed, with the aim of gaining an in-depth understanding of the distribution, temporal patterns and intensity of fires in Riau Province. This approach utilizes filtered hotspot data to generate more accurate insights into the dynamics of fires in tropical peat ecosystems. Riau Province was chosen because it is one of the regions with the highest incidence of peat fires in Indonesia, especially during the dry season [9]. The analysis includes spatial mapping, daily hotspot calculations, temporal FRP evaluation and measurement of fire persistence at the grid level.

Hotspots were mapped using a Geographic Information System (GIS) approach through the Cartopy library in Python to visually describe spatial distribution and identify areas prone to recurrent fires. This mapping enabled visualization of hotspot concentrations in the Riau Province peatland area, including cluster patterns during the observation period. The mapping results highlight priority zones that frequently experience fire activity, assisting in mitigation planning. The Cartopy approach was chosen for its ability to produce high-quality maps with accurate geographic projections. Thus, this initial step provides a basis for more detailed temporal analysis. The number of hotspots was then calculated daily to reveal daily fire activity trends using equation (1).

$$H_d = \sum_{i=n}^{n} I_I \tag{1}$$

Where H_d is the number of hotspots on day *d*, I_I is 1 if a hotspot is detected and *0* if not and n is the total number of hotspots recorded on that day. This calculation identifies peak fire periods during the dry season in Riau Province, often associated with extreme drought conditions [2]. Daily hotspot analysis provides important information about fluctuations in fire activity on a short time scale. The results can support the development of early warning systems for communities and stakeholders. This approach is a standard method in satellite fire monitoring studies to capture temporal dynamics. Next, the intensity of the fire is evaluated through the total, average and maximum FRP calculated daily and monthly using equation (2).

$$FRP_d = \sum_{i=n}^{n} FRP_i \tag{2}$$

Where FRP_d is the total FRP on day *d*, FRP_i is the FRP value for each individual hotspot and n is the number of daily hotspots. This temporal FRP analysis shows variations in fire intensity throughout the season, with high values often occurring during the smoldering phase of peat fires [1]. FRP is a strong indicator for carbon emission estimates because it correlates with the energy released during combustion [5]. The identified seasonal patterns help link fire intensity to environmental factors such as low rainfall. Finally, fire persistence is measured at the grid level to detect areas with recurring events using equation (3).

$$P_g = \sum_{d=1}^{D} A_{g,d} \tag{3}$$

Where P_g is the persistence on grid g, $A_{g,d}$ is 1 if a hotspot exists on day *d* and grid *g* and *0* otherwise and *D* is the total number of observation days. This analysis effectively identifies priority located for restoration in Riau Province, as recurrent fires on peatlands disrupt vegetation recovery and increase long-term emissions [1]. Repeated

fires in peat ecosystems have a significant impact on carbon balance and forest recovery, as discussed in a research on the cycle of repeated fires in Indonesian peatlands [1]. By focusing on grid persistence, this research highlights areas that require urgent restoration intervention. This process refines the holistic analysis of fire risk and supports sustainable land management strategies in the province.

E. Statistical Analysis and Emission Estimation

Statistical thresholds were applied to identify extreme fire days based on the 90th and 95th percentiles (P90 and P95) of the daily FRP distribution, enabling the characterization of high-intensity periods with significant implications for air quality and public health [17]. CO_2 emissions were estimated using FRP as a proxy for biomass consumption, multiplied by appropriate conversion coefficients and emission factors, to quantify the environmental impact of detected fires and support recommendations for peatland restoration and climate change mitigation [5]. The emission estimation follows a simplified FRP based formulation where carbon emissions are calculated by converting Fire Radiative Power into biomass combustion and multiplying it by the CO_2 emission factor. The equation can be expressed as equation (4).

$$E_{CO2} = FRP \times CF \times EF_{CO2} \quad (4)$$

It should be noted that the conversion factor (CF) and emission factor ($EFCO_2$) used in this research are derived from general literature and are not specifically calibrated for peatland conditions in Riau Province. As a result, the emission estimates may contain inherent uncertainties related to variations in peat characteristics, combustion efficiency, and moisture content. This FRP based approach has been demonstrated effective for estimating carbon loss across various vegetation types in tropical and subtropical regions, reinforcing its applicability to peatland fire studies [5].

III. RESULTS AND DISCUSSION

A. Spatiotemporal Distribution of Peatland Fire Hotspots

Based on the results of preprocessing and initial spatial distribution evaluation, further analysis focused on selecting key hotspots that represent high-intensity peatland fires and have a high level of detection reliability. This selection was made by applying two main criteria, namely a confidence level ≥ 70% and FRP ≥ 5 MW. The confidence level criterion was used to minimize the possibility of false detection, while the FRP threshold was maintained to ensure that the hotspots analyzed reflected a physically significant release of fire energy.

Figure 2 shows the spatial distribution of major peatland fire hotspots in Riau Province for the period July–October 2025. It shows a dense concentration in the eastern and central coastal areas of the province. This spatial concentration is likely associated with the extensive distribution of peatland ecosystems in the coastal lowlands of Riau Province, where drainage canals and agricultural expansion may reduce groundwater levels and increase peat dryness, making these areas more susceptible to fire during the dry season.

A total of 7,297 significant hotspots with confidence ≥70% and FRP ≥5 MW were detected using the NASA FIRMS multisensor approach, with red-orange dots representing FRP intensities ranging from low to high, up to >250 MW. The densest clusters were observed around the coordinates 1.9°N–2.1°N and 100.4°E–100.7°E, as well as 1.2°N–1.5°N and 99.7°E, reflecting degraded peatland areas that are prone to repeated burning during the dry season. The pronounced clustering in these areas is strongly associated with extensive canal drainage networks and large-scale oil palm concessions, which lower the peat water table and increase flammability, particularly in zones that have undergone long-term degradation. These locations often correspond to failed or incomplete peat restoration efforts, where rewetting infrastructure is either absent or insufficient, thereby sustaining recurrent smoldering fires.

A significant accumulation of hotspots was observed around the flood-prone zone marked with a cyan star (★) at coordinates approximately 101.44°E, 0.51°N. Clusters of hotspots with high FRP >150–250 MW to the north and southwest of these locations indicate smoldering fires typical of peatlands, which can exacerbate post-fire hydrological vulnerability through peat structure degradation, reduced water retention capacity and increased surface runoff. This spatial proximity underscores a direct causal link between intense dry-season burning and elevated flood risk during the subsequent wet season, as degraded peat loses its natural sponge-like capacity and accelerates overland flow. This pattern suggests a potential relationship between intense dry season fires and the risk of flooding in November–December 2025, in line with the impact of peat degradation on local hydrology.

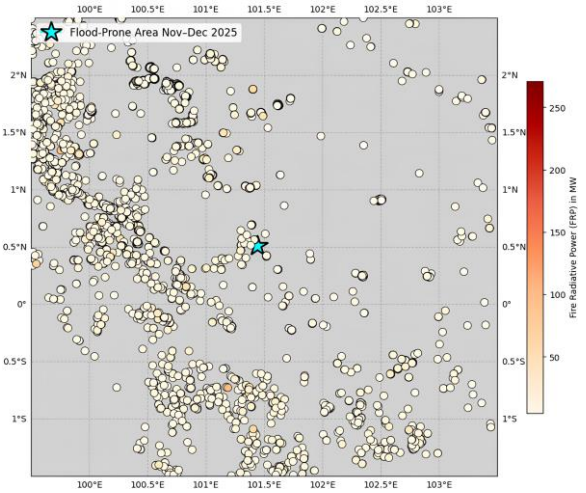

Figure 2. Spatial distribution of filtered hotspots in Riau Province.

The total number of significant hotspots was calculated after deduplication of overlapping detections between sources at the same coordinates and time and the application of a confidence threshold of ≥70% and an FRP of ≥5 MW. Because the dataset integrates multiple satellite observations from the NASA Fire Information for Resource Management System platform, duplicate detections may occur when the same fire is recorded by different sensors. Therefore, deduplication was performed to remove overlapping records with similar coordinates and acquisition times, ensuring that each fire event is counted only once and improving the reliability of hotspot statistics in Riau Province. The temporal pattern of fire activity is further explained through the daily hotspot count graph in Figure 3.

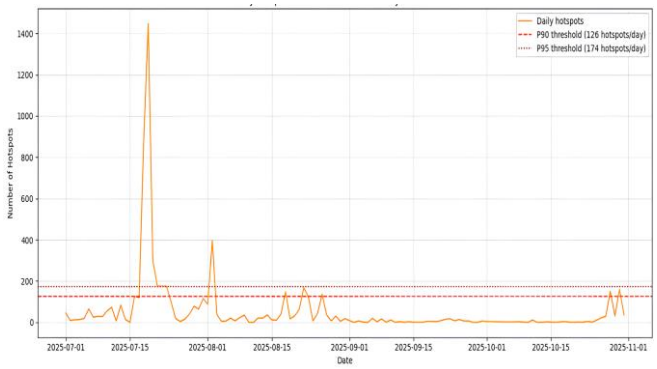

Figure 3. Daily hotspot count during July–October 2025.

The number of hotspots peaked in mid-July 2025 with more than 1,400 points in a single day, far exceeding the P90 threshold of 126 hotspots/day and P95 threshold of 174 hotspots. This peak likely corresponds to the period of maximum seasonal drought in peatland ecosystems, when prolonged dry conditions reduce soil moisture and facilitate the spread of surface and smoldering fires. Although meteorological data were not directly integrated in this research, the observed fire peaks in July are consistent with known seasonal drought patterns in Sumatra. During this period, reduced rainfall and lower humidity levels significantly increase peatland flammability, accelerating both surface and subsurface fire propagation. This spike was followed by a sharp decline, then a secondary wave in early August of around 400 hotspots and minor fluctuations until the end of October. After mid-August, hotspot activity generally remained below the P90 threshold, signaling a transition to the wet season with a significant decrease in fire intensity.

Extreme days were predominant at the beginning of the dry season, with the number of hotspots substantially exceeding P95 on several critical days. These days correlated with extreme dry weather conditions that accelerated the spread of fire on degraded peatlands. The P90 and P95 thresholds set from the data distribution successfully identified periods of high risk for smoke emissions and public health impacts, as seen from the clear separation between normal and extreme days in the graph. This pattern confirms that peatland fires in Riau Province tend to be concentrated in the early dry season before rainfall gradually increases. Figure 4 shows an extraordinary spike in mid-July 2025, with a peak value of 25,611.4 MW in a single day, much higher than on other days.

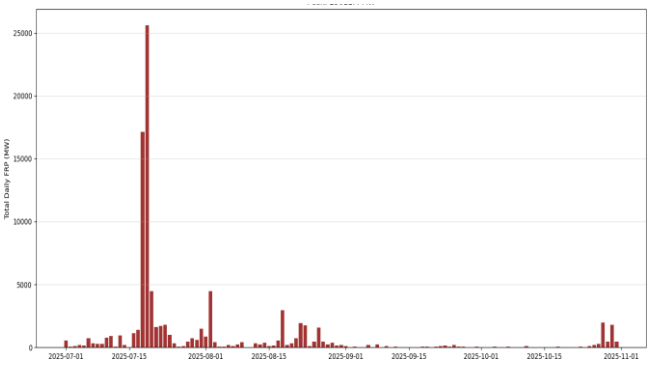

Figure 4. Daily FRP time series showing fire intensity accumulation.

This extreme peak was preceded by a period of intense accumulation that had been increasing since the end of June, followed by a phase of high intensity that remained significant until early August, with many days recording daily FRP totals between 5,000 and 15,000 MW. This indicates that large-scale, sustained fires occurred in succession, possibly driven by prolonged drought conditions combined with human land management activities that allow fires to spread across drained peatland landscapes.

After early August, FRP values declined sharply and consistently towards the end of September, reaching almost zero in October at the end of the dry season. Small fluctuations still detected in the final period indicate that the vulnerability of degraded peatlands to fire remains, even though air humidity conditions have improved.

This pattern clearly illustrates that very high-intensity fires are concentrated in the early phase of the dry season, when extreme drought strongly supports large-scale peat burning. The dominance of FRP on peak days reflects the characteristic smoldering fires typical of degraded peatlands, which contribute significantly to long-term carbon emissions and hydrological degradation.

Overall, the daily FRP distribution as seen in the histogram is highly right-skewed most hotspots have low to moderate FRP <25 MW, while only a few hotspots with very high FRP >50–175 MW dominate the total radiative energy released, especially during the peak period of July–August. This pattern is typical of peatland fire regimes, where numerous small surface fires coexist with fewer but more intense smoldering fires that release large amounts of radiative energy. The highest peak of 25,611 MW is most likely related to massive fires caused by land clearing or uncontrolled burning in priority peatland restoration areas. The drastic decline after August is a natural response to

increased humidity, but the persistent vulnerability of damaged peatlands remains a major concern. Figure 5 shows a graph of monthly total FRP revealing a highly uneven distribution of fire intensity.

With a marked dominance in July reaching 65,120 MW, it was much higher than in the following months. This overwhelming dominance in July can be attributed to the combination of seasonal drought, low soil moisture and anthropogenic burning activities that are typically concentrated at the beginning of the dry season before regulatory enforcement or rainfall suppression becomes effective. August still contributed substantially with 19,886 MW, while September dropped dramatically to only 1,647 MW, before increasing again in October to 5,793 MW. This pattern indicates that the majority of fire energy is concentrated in the early phase of the dry season, when extreme drought conditions allow for large-scale burning of open and degraded peatlands.

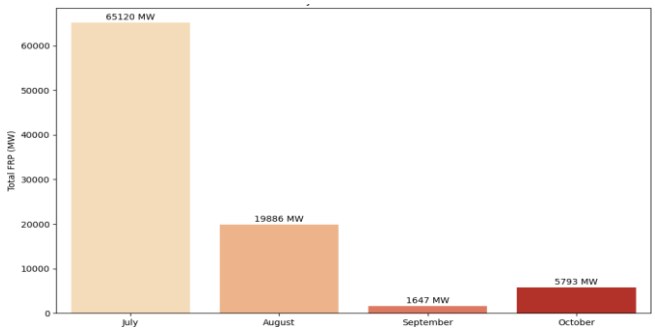

Figure 5. Monthly total FRP for the research period.

Extreme monthly imbalances are evident, with July contributing nearly 70% of the total FRP for the entire period, while September recorded the lowest value. The rebound in October signals significant late-season fire activity, likely related to residual burning or continued land clearing before the rainy season. The dominance of FRP in July reflects massive fire episodes that contributed greatly to carbon emissions and peat degradation, while the sharp decline in September confirms the influence of increased early humidity on natural fire suppression. This pattern reinforces the importance of selecting high FRP-based hotspots to isolate periods of highest risk in emissions and environmental impact analysis. Overall, the spatial clustering and temporal peaks observed in July suggest that peatland degradation, drainage systems and seasonal drought conditions jointly play an important role in shaping fire dynamics in Riau Province.

B. Fire Intensity Characteristics (FRP Analysis)

To further examine the right-skewed distribution of fire radiative power, values were classified into three intensity categories consisting of low intensity between 5 and 25 MW, moderate intensity between 25 and 75 MW, and high intensity exceeding 75 MW. Although high-intensity hotspots account for less than 10 percent of total detections, they contribute more than 60 percent of total radiative energy. Analysis of fire intensity accumulation ahead of the late wet season from September to October 2025 as shown in Figure 6 reveals a striking pattern, with daily fire radiative power remaining relatively low and stable below 300 MW throughout September to mid-October before surging sharply toward the end of October and early November. The highest peak was recorded during this late period, reaching between 1,800 and 2,000 MW for several consecutive days followed by a rapid decline. This late-season surge likely reflects residual drying of surface peat layers combined with persistent smoldering in deeper peat, which can continue even under marginal moisture conditions before full monsoon onset. This final surge indicates the last episode of intense fires before the transition to the rainy season, which was most likely triggered by residual dry conditions and dry winds that still supported the spread of fire on peatlands.

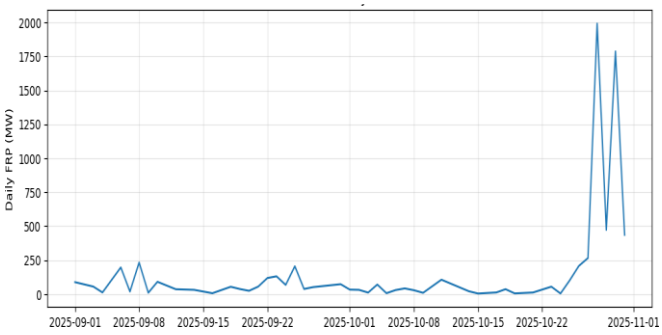

Figure 6. Sharp increase in daily FRP at the end of October 2025.

The main findings indicate that fire activity was dominant during the early phase of the dry season in July 2025, with daily hotspot counts reaching several hundred detections and substantial accumulation of FRP. Fire activity gradually declined from September to mid-October, indicating a transition toward wetter seasonal conditions. Persistence analysis shows that several 0.1° grid cells experienced fire activity for up to 21 days during the observation period, particularly around lat_bin 1.2, lon_bin 99.7 and lat_bin 1.9, lon_bin 99.8. These persistent grids highlight areas of deep peat where smoldering combustion can sustain for weeks, releasing substantial latent heat and contributing disproportionately to total carbon loss even when surface hotspot counts decrease. These areas represent peatland zones that are prone to repeated burning, where smoldering combustion can persist even when daily hotspot intensity decreases.

Overall, the pattern shows a concentration of peatland fires in Riau Province in July 2025, followed by a post-August decline, with residual risk at the end of the season. Compared to previous studies in Sumatra that primarily relied on hotspot counts, this research provides a more detailed perspective by incorporating FRP-based intensity analysis. Earlier studies often reported peak fire

activity in August–September, whereas this research identifies an earlier peak in July, suggesting a potential shift in seasonal fire dynamics and highlighting the importance of intensity-based analysis. The FRP distribution, which is heavily skewed to the right, indicates that a small number of extreme hotspots dominate radiative energy, while high persistence in certain grids indicates areas of recurrent fires. This right-skewed FRP distribution is characteristic of peatland fires, where a minority of high-intensity smoldering hotspots often >100 MW account for the majority of total fire radiative energy and biomass consumption, thereby amplifying potential greenhouse gas emissions far beyond what surface hotspot counts alone would suggest. This pattern is consistent with the characteristics of smoldering tropical peat, although satellite data cannot directly measure the depth of burning. Extreme weather conditions such as maximum temperatures of 36 °C, minimum humidity of 37% and temperature rise rates of 2.7 °C/hour as observed in Central Kalimantan [20], likely contributed to the intensification of fires in the early and late dry phases. This is also in line with the trend of drought amplification of up to 60% in southern Indonesia.

However, satellite analysis has limitations, including the potential for false positives even when confidence ≥70% and FRP ≥5 MW are applied. The identified temporal and spatial patterns indicate the potential risk of late-season flare-ups and recurrent fires in coastal zones near flood-prone areas, which may affect post-fire hydrology. Fire prevention in post-2015 managed landscapes has shown a decline in fire activity, while bundles of sanctions-based interventions and health concerns may be adaptive options. Restoration considerations also need to include economic trade-offs. A multisensor time series approach provides additional information compared to static analysis, but real-time weather data integration and field validation are still needed for more accurate mitigation recommendations in Riau Province peatlands.

C. Carbon Emission Implications of Peatland Fires

The distribution of FRP for 7,297 major peatland fire hotspots in Riau Province in 2025 shows a highly right-skewed distribution pattern. More than 1,300 hotspots have low to moderate FRP values in the range of 5–25 MW, reflecting the dominance of fires with relatively low to moderate intensity during the observation period. Conversely, extreme values above 75 MW were only identified in a small number of points, with a maximum value of around 175 MW. The overall average FRP was recorded at 13.2 MW and was located near the lower portion of the distribution, indicating that the mean value is influenced by a small number of very high-intensity hotspots. This pattern indicates that although low-intensity fires occur more frequently, a limited number of high-intensity events contribute disproportionately to the total radiative energy released. Such characteristics are typical of tropical peatland fires, where smoldering combustion can persist for long durations and occasionally generate very high FRP values detected by satellite observations.

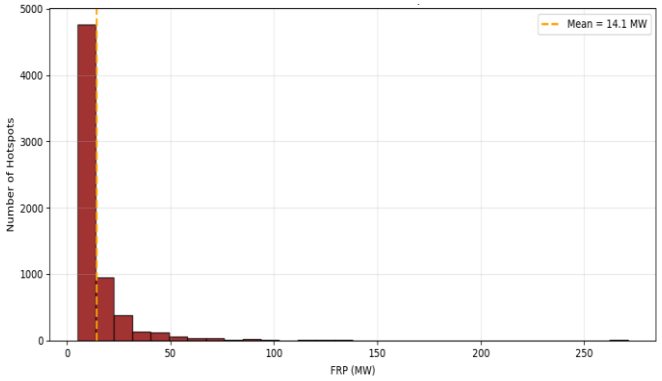

Figure 7. Right-skewed distribution of hotspot FRP values.

This asymmetric distribution phenomenon has important implications for statistical analysis and emission estimation, as the use of average values alone has the potential to mask the dominant characteristic of numerous low-intensity fires with high frequency. Therefore, FRP interpretation needs to consider the overall data distribution, including the presence of high-intensity outliers that contribute significantly to the total FRE. This right-skewed distribution pattern is shown in Figure 7, which shows a concentration of frequencies in the low to medium FRP classes and a long tail in the high FRP values.

The statistical approach combining FRP distribution analysis with a selection threshold of ≥5 MW effectively isolated the main contributors to emissions. By focusing on high FRP hotspots, this method provides a more representative basis for estimating CO_2 emissions, because a few extreme hotspots may contribute disproportionately to the total radiative energy released during the research period. These results not only reinforce the validity of using FRP as a proxy for biomass consumption and support environmental risk assessment related to peatland fires. In the context of Indonesian peatland management, these findings offer significant practical contributions as a guide for prioritizing intensive monitoring and rapid intervention in high-intensity hotspots, thereby reducing disproportionate carbon emissions and improving regional air quality. The observed distribution pattern suggests a systematic characteristic of dry-season fire dynamics, where frequent low-intensity fires coexist with less frequent but energetically significant high-intensity events.

The Mann-Whitney U test conducted to compare the distribution of FRP on days with high smoke intensity, FRP >100 MW and low non-smoke days produced a highly significant p-value of 5.45×10^{-22}. These results confirm a clear and strong difference between the two groups, with days with high FRP showing much greater emission intensity. These findings reinforce that episodes of

high-intensity fires are not merely sporadic events, but contribute significantly to total emissions and environmental impacts during the research period.

Finally, the ten hottest hotspots in Riau Province in 2025 showed the highest fire intensity reaching 189.4 MW, followed by three other hotspots with FRP of 134.6 MW and several others in the range of approximately 111–126 MW. These ten hotspots contributed to a very high FRP value, far above the overall average of 13.2 MW. This is shown in Figure 8.

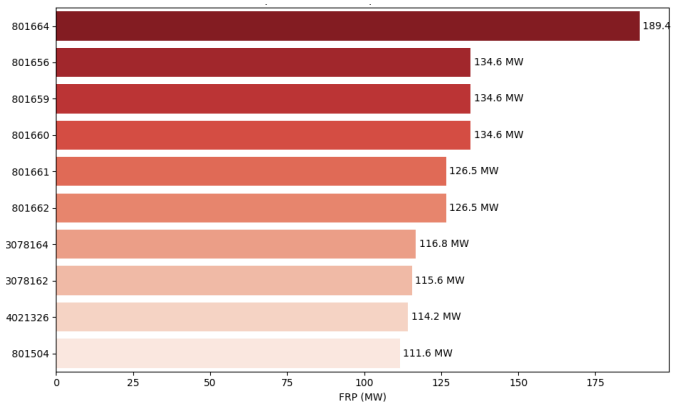

Figure 8. Top 10 highest-intensity hotspots with maximum FRP.

Bounding on the FRP characteristics described in the previous section, this section focuses on deriving carbon emission estimates from fire intensity indicators and discusses their broader environmental implications in the context of peatland fires in Riau Province.

The right-skewed FRP distribution, with an average of 13.2 MW and extremes up to 189.4 MW, implies that low-intensity fires dominate in number while a small number of high-FRP hotspots especially those >75 MW drive the majority of FRE, biomass consumption and CO_2 emissions. To quantify this, emission estimates were derived by integrating FRP time-series into FRE, then applying peat-specific conversion factors to estimate biomass burned and CO_2 released. This outlier-focused method provides a more accurate representation of total emissions than mean-based approaches alone.

The overall findings from this spatial-temporal and statistical analysis underscore the dominance of early dry season fires and the risk of late season flare-ups on Riau Province peatlands, with significant implications for emissions, public health [17], and the need for integrated interventions. Sanction-based prevention and health concerns [21], combined with restoration that considers economic trade-offs [22], as well as successful prevention in managed landscapes [23], are key to reducing future fire activity, especially amid extreme weather conditions. Although direct field validation was not conducted, the results obtained in this research are consistent with previous satellite-based fire analyses and national fire monitoring reports. This consistency supports the reliability of the multisensor FIRMS dataset in capturing peatland fire dynamics in Riau Province.

D. Uncertainty and Error Assessment in Fire Detection

The analysis of peatland fire hotspots in Riau Province relies on multisensor satellite observations and FRP-based proxies for fire intensity and carbon emissions, which inherently introduce several sources of uncertainty. Potential errors include misclassification of hotspots due to cloud cover, smoke interference, or sensor-specific detection limits, as well as temporal gaps in satellite coverage that may fail to capture short-lived or transient fire events. While the application of a confidence threshold ≥70% and FRP ≥5 MW reduces the likelihood of false positives and focuses the analysis on significant fires, residual uncertainties persist, particularly for low-intensity or patchy fires that could cumulatively contribute to emissions but remain underrepresented in the dataset. These uncertainties highlight the need for cautious interpretation of emission estimates and spatial–temporal patterns, particularly in areas with heterogeneous peat conditions.

A further source of error lies in the conversion of FRP to biomass consumption and CO_2 emissions, which relies on assumptions about peat characteristics, combustion completeness and carbon content. Variations in peat depth, moisture and degradation state are not directly measurable via satellite data, meaning that emission estimates may either overestimate or underestimate actual carbon release. These uncertainties are compounded in areas with repeated smoldering fires, where residual heat can persist undetected and in marginal peatlands with mixed soil types. Future research should include field validation, high-resolution satellite data and potentially modeling approaches such as machine learning-based fire prediction to refine hotspot identification and improve FRP-to-emission conversion accuracy.

IV. CONCLUSION

This research analyzes the characteristics of peatland fires in Riau Province during the dry season from July to October 2025 using NASA FIRMS multisensor data MODIS and VIIRS from the Suomi-NPP, NOAA-20 and NOAA-21 satellites. After spatial and temporal filtering, 7,297 hotspots with a confidence level of ≥70% and FRP ≥5 MW were identified, with peak activity occurring in July with a maximum daily FRP of 25,611 MW and a monthly total of 65,120 MW. Fire activity then declined substantially in September to approximately 1,647 MW before showing a moderate increase again in October to early November, with daily FRP values ranging between 1,800 and 2,000 MW. The distribution of FRP values was highly right-skewed with a mean of 13.2 MW, indicating that a relatively small fraction of high intensity hotspots contributed disproportionately to the total radiative energy release.

High-intensity hotspots were identified around coordinates 101.44°E, 0.51°N, which are spatially close to flood-prone areas. Persistence analysis indicates repeated fire occurrences in these high-risk zones, suggesting dominant spatial patterns and potential post-fire hydrological vulnerability. Limitations of this research include the lack of integration of high-resolution hydrometeorological data, measurement of burn depth and field validation. However, this research is limited to a single dry-season period (July–October 2025), which may not fully capture interannual variability influenced by climatic phenomena such as El Niño or La Niña. Additionally, uncertainties remain in FRP-based emission estimation due to variations in peat depth, moisture conditions and combustion completeness, which may affect the accuracy of carbon emission estimates.

Future research should integrate high-resolution satellite imagery, machine learning-based fire prediction models, real-time weather data and hydrological modeling to enhance fire risk assessment accuracy and support evidence-based peatland management strategies. Furthermore, the use of multi-year datasets and field-based validation is strongly recommended to improve the robustness, generalizability and reliability of the findings.

REFERENCES

[1] H. Krisnawati *et al.*, "Building capacity for estimating fire emissions from tropical peatlands; a worked example from Indonesia," *Sci. Rep.*, vol. 13, no. 1, p. 14355, Sep. 2023, doi: 10.1038/s41598-023-40894-z.

[2] H. Hayasaka, "Peatland Fire Weather Conditions in Sumatra, Indonesia," *Climate*, vol. 11, no. 5, p. 92, Apr. 2023, doi: 10.3390/cli11050092.

[3] M. J. Wooster *et al.*, "Satellite remote sensing of active fires: History and current status, applications and future requirements," *Remote Sens. Environ.*, vol. 267, p. 112694, Dec. 2021, doi: 10.1016/j.rse.2021.112694.

[4] L. Kiely *et al.*, "Assessing costs of Indonesian fires and the benefits of restoring peatland," *Nat. Commun.*, vol. 12, no. 1, p. 7044, Dec. 2021, doi: 10.1038/s41467-021-27353-x.

[5] M. Parrington *et al.*, "Biomass burning emission estimation in the MODIS era: State-of-the-art and future directions," *Elem Sci Anth*, vol. 13, no. 1, p. 00089, Sep. 2025, doi: 10.1525/elementa.2024.00089.

[6] X. Lu, X. Zhang, F. Li, and M. A. Cochrane, "Improved estimation of fire particulate emissions using a combination of VIIRS and AHI data for Indonesia during 2015–2020," *Remote Sens. Environ.*, vol. 281, p. 113238, Nov. 2022, doi: 10.1016/j.rse.2022.113238.

[7] C. B. Engel, S. D. Jones, and K. J. Reinke, "Fire Radiative Power (FRP) Values for Biogeographical Region and Individual Geostationary HHMMSS Threshold (BRIGHT) Hotspots Derived from the Advanced Himawari Imager (AHI)," *Remote Sens.*, vol. 14, no. 11, p. 2540, May 2022, doi: 10.3390/rs14112540.

[8] D. A. Tinoco-Orozco *et al.*, "Where Do Fires Burn More Intensely? Modeling and Mapping Maximum MODIS Fire Radiative Power from Aboveground Biomass by Fuel Type in Mexico," *Fire*, vol. 8, no. 2, p. 54, Jan. 2025, doi: 10.3390/fire8020054.

[9] M. Ohashi *et al.*, "Correlation of publication frequency of newspaper articles with environment and public health issues in fire-prone peatland regions of Riau in Sumatra, Indonesia," *Humanit. Soc. Sci. Commun.*, vol. 8, no. 1, p. 307, Dec. 2021, doi: 10.1057/s41599-021-00994-5.

[10] V. S. A. Hendrawan, A. P. Rahardjo, H. G. Mawandha, E. Aldrian, A. Muhari, and D. Komori, "Review article: Past and future climate–related hazards in Indonesia," Jun. 10, 2025, *Atmospheric, Meteorological and Climatological Hazards*. doi: 10.5194/egusphere-2025-584.

[11] E. Wulandari, D. Mardiatno, D. H. Susilastuti, and A. Maryudi, "Scholarly Interest in Forest Fires in Indonesia: A Bibliographical Review," *For. Soc.*, vol. 6, no. 2, pp. 609–619, Aug. 2022, doi: 10.24259/fs.v6i2.21473.

[12] Y. Vetrita *et al.*, "Monthly mapping of Indonesia's burned areas: implementation, history, techniques, and future directions," *Int. J. Remote Sens.*, vol. 46, no. 2, pp. 636–660, Jan. 2025, doi: 10.1080/01431161.2024.2421942.

[13] D. A. Shofiana and I. S. Sitanggang, "Confidence Analysis of Hotspot as Peat Forest Fire Indicator," *J. Phys. Conf. Ser.*, vol. 1751, p. 012035, Jan. 2021, doi: 10.1088/1742-6596/1751/1/012035.

[14] G. McAvoy and K. Vadrevu, "Spatiotemporal Analysis of Vegetation Fires and Carbon Monoxide Pollution in Indonesia," *Remote Sens.*, vol. 17, no. 19, p. 3275, Sep. 2025, doi: 10.3390/rs17193275.

[15] A. M. Graham *et al.*, "Updated Smoke Exposure Estimate for Indonesian Peatland Fires Using a Network of Low-Cost $PM_{2.5}$ Sensors and a Regional Air Quality Model," *GeoHealth*, vol. 8, no. 11, p. e2024GH001125, Nov. 2024, doi: 10.1029/2024GH001125.

[16] H. Purnomo *et al.*, "Community-based fire prevention and peatland restoration in Indonesia: A participatory action research approach," *Environ. Dev.*, vol. 50, p. 100971, Jun. 2024, doi: 10.1016/j.envdev.2024.100971.

[17] M. J. Grosvenor *et al.*, "Catastrophic impact of extreme 2019 Indonesian peatland fires on urban air quality and health," *Commun. Earth Environ.*, vol. 5, no. 1, p. 649, Nov. 2024, doi: 10.1038/s43247-024-01813-w.

[18] D. Fisher, M. J. Wooster, W. Xu, G. Thomas, and P. Lestari, "Top-Down Estimation of Particulate Matter Emissions from Extreme Tropical Peatland Fires Using Geostationary Satellite Fire Radiative Power Observations," *Sensors*, vol. 20, no. 24, p. 7075, Dec. 2020, doi: 10.3390/s20247075.

[19] M. J. Grosvenor *et al.*, "Catastrophic impact of extreme 2019 Indonesian peatland fires on urban air quality and health," *Commun. Earth Environ.*, vol. 5, no. 1, p. 649, Nov. 2024, doi: 10.1038/s43247-024-01813-w.

[20] A. Usup and H. Hayasaka, "Peatland Fire Weather Conditions in Central Kalimantan, Indonesia," *Fire*, vol. 6, no. 5, p. 182, Apr. 2023, doi: 10.3390/fire6050182.

[21] R. Carmenta, A. Zabala, B. Trihadmojo, D. Gaveau, M. A. Salim, and J. Phelps, "Evaluating bundles of interventions to prevent peat-fires in Indonesia," *Glob. Environ. Change*, vol. 67, p. 102154, Mar. 2021, doi: 10.1016/j.gloenvcha.2020.102154.

[22] S.-M. Jalilov, Y. Rochmayanto, D. C. Hidayat, J. T. Raharjo, D. Mendham, and J. D. Langston, "Unveiling economic dimensions of peatland restoration in Indonesia: A systematic literature review," *Ecosyst. Serv.*, vol. 71, p. 101693, Feb. 2025, doi: 10.1016/j.ecoser.2024.101693.

[23] S. Sloan, L. Tacconi, and M. E. Cattau, "Fire prevention in managed landscapes: Recent success and challenges in Indonesia," *Mitig. Adapt. Strateg. Glob. Change*, vol. 26, no. 7, p. 32, Oct. 2021, doi: 10.1007/s11027-021-09965-2.